Formation of bimetallic Rh-Mo crystallites supported on SiO_2 by decomposition of a heteronuclear cluster precursor

R. Lamber, N.I. Jaeger

Institut für Angewandte und Physikalische Chemie, Universität Bremen, W-2800 Bremen, Germany

A. Trunschke and H. Miessner

Zentralinstitut für Physikalische Chemie, Rudower Chaussee 5, O-1199 Berlin, Germany

Received 14 June 1991; accepted 25 July 1991

$Rh\text{-}Mo/SiO_2$ catalysts prepared from the heteronuclear $(C_5H_5)_3RhMo_2(CO)_5$ precursor were characterized by methods of analytical electron microscopy. The formation of bimetallic Rh-Mo crystallites with f.c.c., b.c.c. and c.p. hexagonal structures similar to those observed in bulk Rh-Mo alloys could be established and related to the outstanding properties of the catalyst.

Keywords: Bimetallic Rh-Mo clusters; $Rh\text{-}Mo/SiO_2$ catalyst; heteronuclear clusters; electron microdiffraction; EDX analysis

1. Introduction

The interest and continued investigation of bimetallic heterogeneous catalysts is due to the fact that they often exhibit improved catalytic activity and selectivity in heterogeneous reactions compared to their monometallic counterparts [1–3]. Recently, heteronuclear clusters have been used as precursors of the metal phase [4–11]. There is microanalytical evidence that this method of preparation can lead to the formation of bimetallic particles [5,6,9].

Recent investigations of molybdenum promoted Rh/SiO_2 catalysts in CO hydrogenation and olefin hydroformylation have shown that catalysts prepared from a $(C_5H_5)_3RhMo_2(CO)_5$ precursor show a marked difference in catalytic activity and selectivity when compared to catalysts prepared from metal salt precursors [7,10]. Thus, due to specific promotion of methanol and ethanol formation together with the suppression of methane production, an unusual high oxygenate selectivity of more than 50 mol% is obtained on the cluster-de-

rived catalyst in syngas conversion [7]. The product distribution gave rise to the assumption of a close contact between the active metal and the promotor on the catalyst surface. In order to elucidate the outstanding properties of the cluster-derived catalyst a characterization by analytical electron microscopy (AEM) was carried out. Results of these investigations are presented in this paper.

2. Experimental procedure

Details of the preparation of the Rh-Mo/SiO_2 catalysts are given in previous papers [7,10,11]. $(C_5H_5)_3RhMo_2(CO)_5$ was deposited onto silica-gel (GR-10301, Fuji-Davison, mesh 20 to 12) from CH_2Cl_2 solution under argon atmosphere. After removing the solvent in vacuum at room temperature the catalyst was gently oxidized in O_2 (flow rate 60 ml min^{-1}) for two hours at 373 K in order to avoid the formation of volatile carbonyls during reduction. Finally, the sample

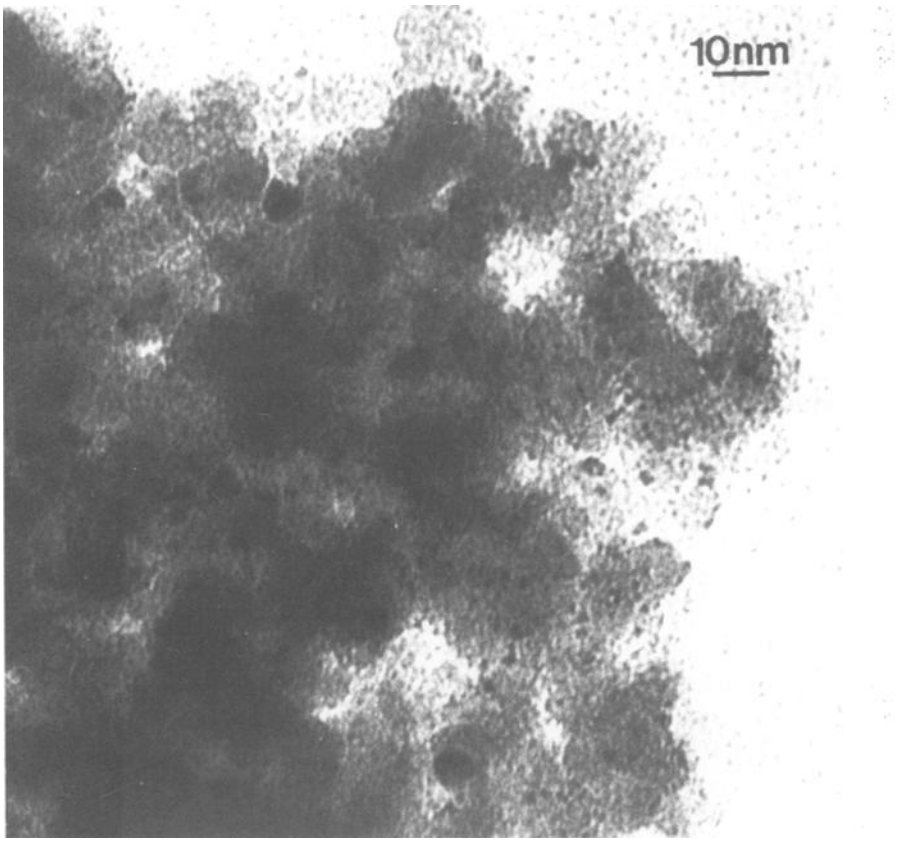

Fig. 1. Representative electron micrograph from the Rh-Mo/SiO_2 catalyst after reduction in H_2 at 673 K.

(1.7 wt.% Rh) was reduced in hydrogen (flow rate 60 ml min^{-1}) for two hours at 673 K. Before the AEM characterization the Rh-Mo/SiO_2 catalyst was ground to a fine powder, deposited on a copper grid coated with a carbon film and dispersed in an ultrasonic bath. No organic solvents were used during this procedure. The catalyst was characterized in a Philips EM 420 T transmission electron microscope (LaB_6 filament) operated at 120 kV and equipped with an energy dispersive X-ray analyzer (EDX). The elemental composition of the metal particles was checked by using EDX with a stationary TEM probe. A large number of individual metal particles 5–7 nm size have been analyzed in the nanoprobe mode with a spot size about 12 nm. Decreasing of the probe size led to counting rates too low due to the lower current in the electron probe. Structural informations from metal particles were derived from nanodiffraction patterns which could be obtained by using a small (5 nm) stationary electron probe.

3. Results

Fig. 1 depicts an electron micrograph obtained from the Rh-Mo/SiO_2 catalyst prepared from the $(C_5H_5)_3RhMo_2(CO)_5$ precursor. The size histogram is shown in fig. 2. By large area EDX analysis (spot diameter ≈ 250 nm) the presence of both Rh and Mo was established. Typical EDX spectra obtained when the electron probe was focussed on the Rh-Mo particles are shown in figs. 3a and 3b. Most of the EDX spectra taken from particle free SiO_2-support

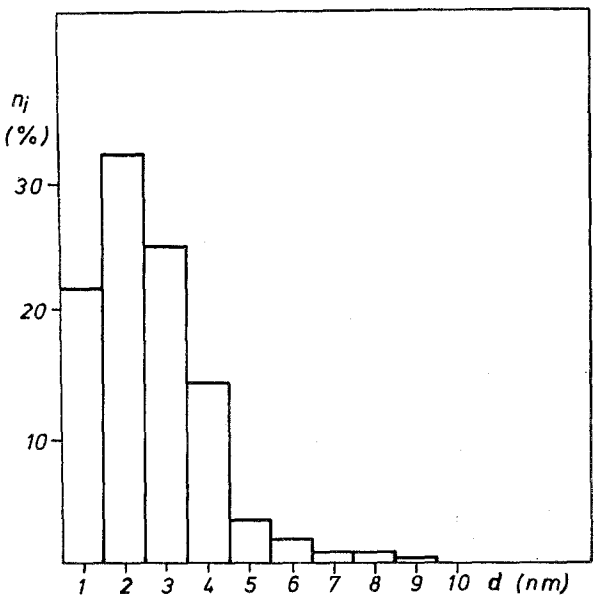

Fig. 2. Particle size distribution from the Rh-Mo/SiO_2 catalyst.

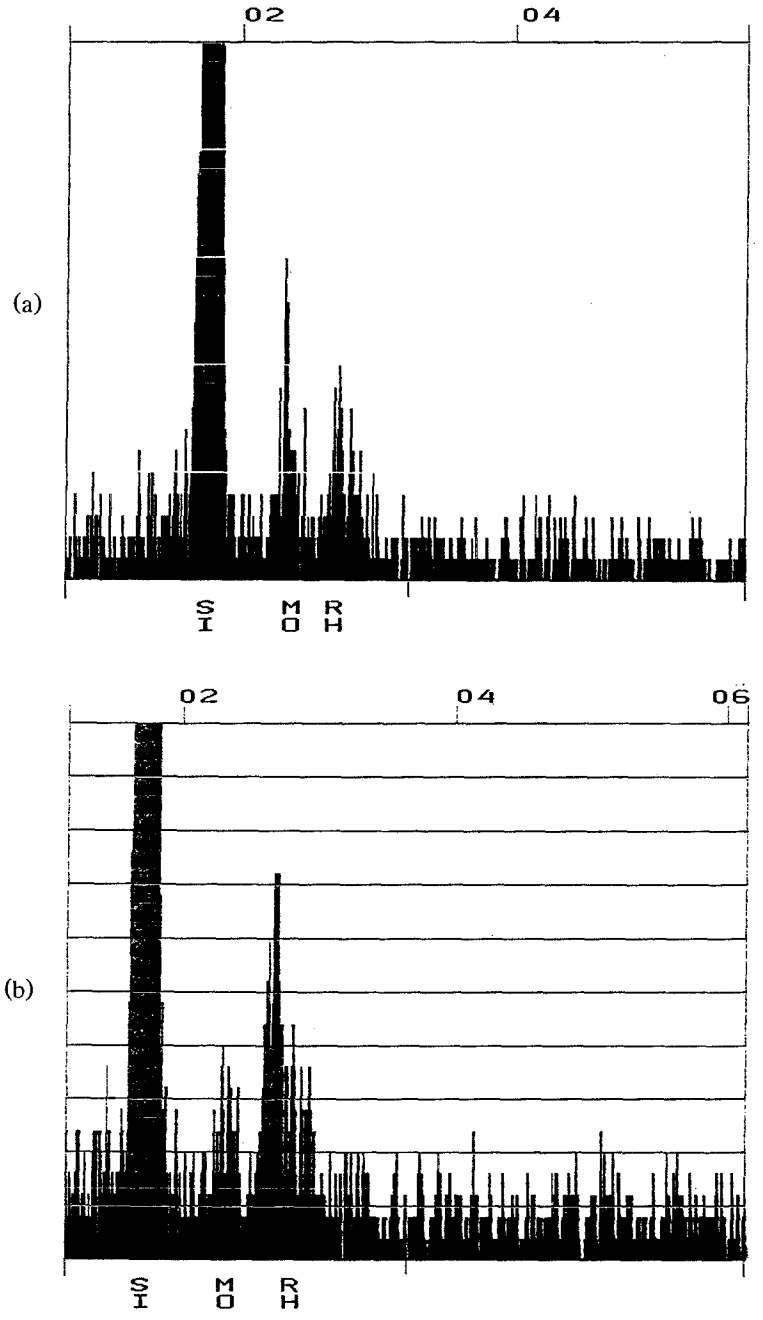

Fig. 3. (a) EDX spectrum from a 6 nm particle. (b) EDX spectrum from a 7 nm particle.

zones did not reveal the presence of either Rh or Mo peaks. In some cases, however, a weak Mo signal was observed. Nanodiffraction analysis of the metal aggregates gave evidence for the presence of Rh-Mo crystallites with different

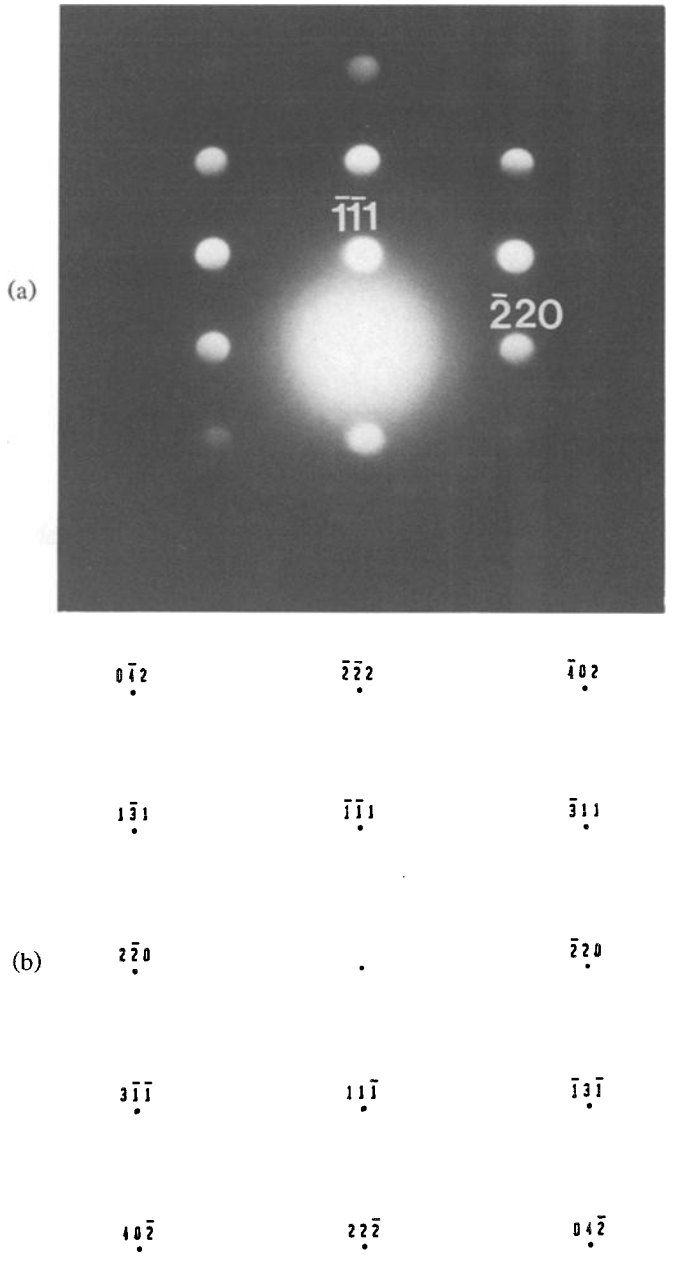

Fig. 4. (a) Nanodiffraction pattern obtained from a 6 nm bimetallic particle with the f.c.c. structure ($a = 0.38$ nm) in the [112] orientation. (b) Interpretation of fig. 4a.

structures. Fig. 4a depicts a nanodiffraction pattern taken from a 6 nm particle. This pattern is typical for a f.c.c. crystallite ($a = 0.38$ nm) in the [112] orientation (fig. 4b). Fig. 5a shows an example of a nanodiffractogram which can be ascribed

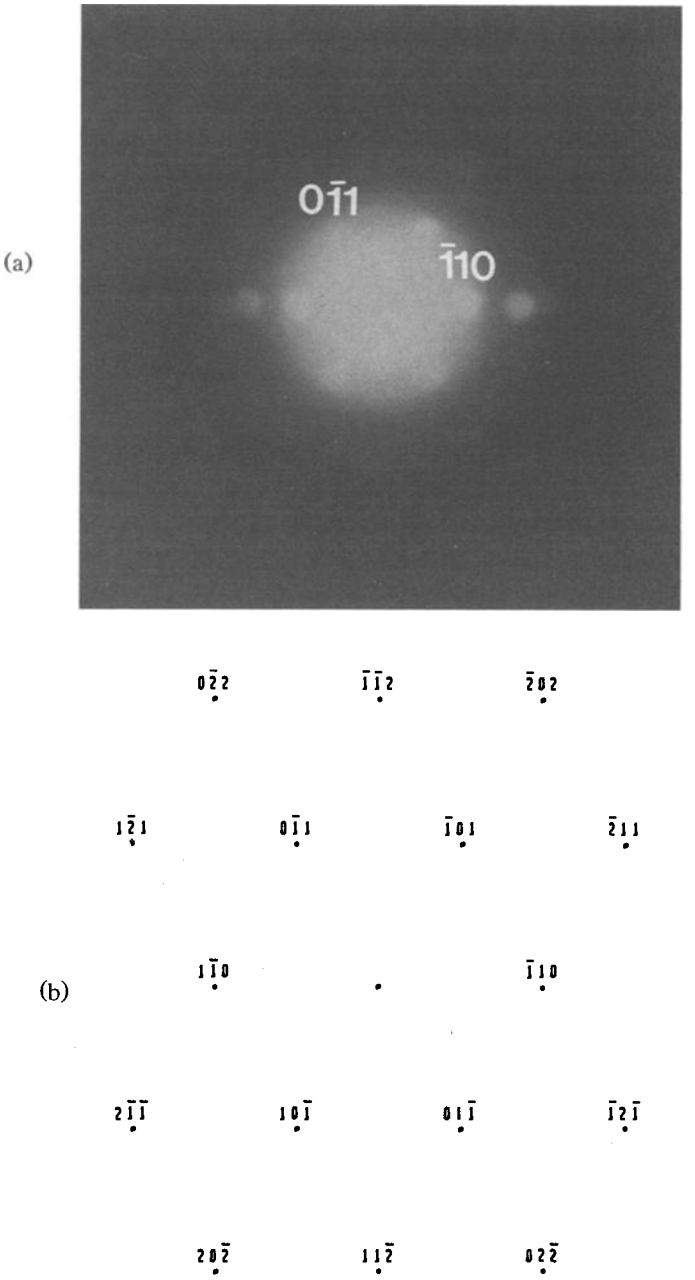

Fig. 5. (a) Nanodiffraction pattern taken from a 4 nm bimetallic aggregate with the b.c.c. structure ($b = 0.31$ nm) in the [111] orientation. (b) Interpretation of fig. 5a.

to a b.c.c. crystal ($a = 0.31$ nm) in the [111] orientation (fig. 5b). The nanodiffraction pattern presented in fig. 6a indicates the presence of particles with the c.p. hexagonal structure ($a = 0.27$ nm, $c = 0.44$ nm). The nanodiffraction

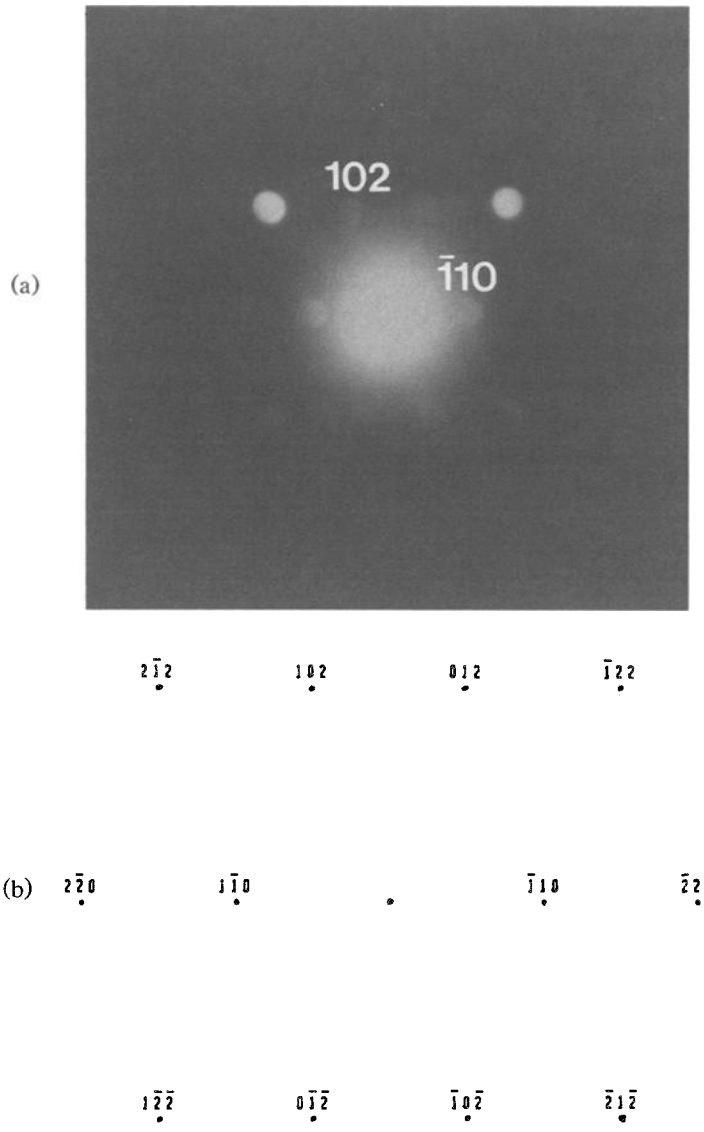

Fig. 6. (a) Nanodiffractogram obtained from a 7 nm crystallite with the c.p. hexagonal structure ($a = 0.27$ nm, $c = 0.44$ nm) in the $[22\bar{1}]$ orientation. (b) Interpretation of fig. 6a.

patterns in fig. 5a and 6a exhibit splitting of some diffraction spots. Spot-splitting in microdiffraction patterns from small metal particles can be caused by: (i) the probe position relative to the small crystal; (ii) the operating conditions of the objective lens; (iii) misalignment of the microscope [12]. The splitting of some spots (fig. 5a and 6a) did not cause unambiguity in determining of the crystal structure. It has to be added that in many cases evidence for the presence

of twinned Rh-Mo aggregates was obtained. No bimetallic particles could be detected by methods of analytical electron microscopy in the case of catalysts derived from mixed metal salt precursors.

It has been found in the catalytic hydroformylation of ethene and propene that the cluster-derived catalyst led to a significant increase in the rate of hydrogenation and hydroformylation [10]. In the hydrogenation of acetaldehyde the highest selectivity for the formation of ethanol was observed for the cluster derived bimetallic catalyst, which provides the required close vicinity of Rh and Mo [10].

4. Discussion

The comparison of the Rh and Mo peak heights obtained for different Rh-Mo crystallites (figs. 3a and 3b) indicates some differences in composition. However, a reliable quantification of the EDX spectra could not be achieved. The small number of counts that could be accumulated under each peak gave rise to large statistical errors. The spatial resolution of the EDX analysis was also low due to relatively large size of the electron probe (≈ 12 nm) in comparison with the size of the analyzed aggregates (5–7 nm). Nevertheless, the observed rather uncertain EDX results concerning differences in composition of the Rh-Mo aggregates seem to be supported by the nanodiffraction analysis. The appearance of the Rh-Mo crystallites with f.c.c., b.c.c. and c.p. hexagonal structures can be explained by the formation of different Rh-Mo phases in analogy to the known bulk phases. A solid solution of up to 15 at% Rh in Mo was found to crystallize in the b.c.c. structure ($a = 0.3147$–0.3132 nm) [13] and a solid solution of up to 15 at% Mo in Rh in the f.c.c. structure ($a = 0.3803$–0.3818 nm) [14]. The observed lattice constants for the fcc and the bcc structures are very close to these of the pure metals. The bimetallic composition of the particles was proven by EDX. A Rh-Mo phase with c.p. hexagonal structure ($a = 0.2733$ nm, $c = 0.4364$ nm) extends from about 45 to 82 at.% Rh [15]. Evidence for the presence of bimetallic Rh-Mo crystallites are provided by the EDX analysis for aggregates of sizes $\geqslant 5$ nm and by the nanodiffraction analysis for crystallites of sizes $\geqslant 3$ nm. No correlation was observed between structures of the particles and their size in the region 3–7 nm. The detection of weak Mo peak on areas of the SiO_2-support free of metal particles might indicate that molybdenum is also scattered over silica, probably in an oxidized form. Oxidized Mo-species could also be responsible for the promotion of the formation of oxygenated products in the CO hydrogenation [16,17]. On the other hand, the prevention of large ensembles of rhodium atoms due to alloy formation will be decisive in the suppression of the structure sensitive methane formation as observed in CO hydrogenation on the $(C_5H_5)_3RhMo_2(CO)_5$-derived catalyst [7].

5. Conclusion

The results provide convincing evidence that the preparation of the Rh-Mo/SiO_2 catalysts from the heteronuclear $(C_5H_5)_3RhMo_2(CO)_5$ precursor leads to the formation of small bimetallic Rh-Mo particles. Different structures of the Rh-Mo crystallites stem from differences in their composition. However, it cannot be excluded that small Rh-Mo aggregates with a given composition can crystallize in different structures. The formation of bimetallic Rh-Mo particles is assumed to be the reason for the differences in the catalytic behavior observed on cluster- and salt-derived catalysts in the CO hydrogenation.

Acknowledgements

The authors thank Professor G. Schulz-Ekloff for helpful discussions and critical reading of the manuscript. Support by the Volkswagenstiftung (AZ: I/64 808) is gratefully acknowledged. A.T. and H.M. acknowledge support by the BMFT (AZ: 423-4005-OSC 258-3).

References

[1] J.H. Sinfelt, J. Catal. 29 (1973) 308.
[2] J.K.A. Clarke and A.C.M. Creaner, Ind. Eng. Chem. Prod., Res. Div. 20 (1981) 574.
[3] P. Braunstein and J. Rosé, in: *Stereochemistry of Organometallic and Inorganic Compounds*, ed. I. Bernal, Vol. III (Elsevier, Amsterdam, 1988).
[4] J.R. Anderson, P.S. Elmes, R.F. Howe and D.E. Mainwaring, J. Catal. 50 (1977) 508.
[5] A. Choplin, L. Huang, A. Theolier, P. Gallezot, J.M. Basset, U. Siriwardane, S.G. Shore and R. Mathieu, J. Am. Chem. Soc. 108 (1986) 4224.
[6] M. Kaminsky, K.J. Yoon, G.L. Geoffroy and M.A. Vannice, J. Catal. 91 (1985) 338.
[7] A. Trunschke, H. Ewald, D. Gutschick, H. Miessner, M. Skupin, B. Walther and H.-C. Böttcher, J. Mol. Catal. 56 (1989) 95.
[8] M. Ichikawa, L.F. Rao, T. Kimura and A. Fukuoka, J. Mol. Catal. 62 (1990) 15.
[9] G. Predieri, P. Maggi, S. Papadopulos, A. Armigliato, S. Bigi and E. Sappo, J. Chem. Soc., Chem. Commun. (1990) 1736.
[10] A. Trunschke, H.-C. Böttcher, A. Fukuoda, M. Ichikawa and H. Miessner, Catal. Lett. 8 (1991) 221.
[11] B. Walther, M. Scheer, H.-C. Böttcher, A. Trunschke, H. Ewald, D. Gutschick, H. Miessner, M. Skupin and G. Vorbeck, Inorg. Chim. Acta 156 (1989) 285.
[12] M. Pan, J.M. Cowley and J.C. Barry, Ultramicroscopy 30 (1989) 385.
[13] C.W. Haworth and W. Hume-Rothery, J. Inst. Metals 87 (1958/59) 265.
[14] E. Anderson and W. Hume-Rothery, J. Less-Common. Met. 2 (1960) 443.
[15] E. Anderson and W. Hume-Rothery, J. Less.-Common. Met. 2 (1960) 19.
[16] A. Fukuoka, T. Kimura and M. Ichikawa, J. Chem. Soc. (1988) 428.
[17] H.-Y. Luo, A.G.T. Bastein, A.A.J.P. Mulder and V. Ponec, Appl. Catal. 38 (1988) 241.